AAC Journals.ASM.org

Fungicidal Mechanisms of Cathelicidins LL-37 and CATH-2 Revealed by Live-Cell Imaging

Soledad R. Ordonez,[a] Ilham H. Amarullah,[a] Richard W. Wubbolts,[b] Edwin J. A. Veldhuizen,[a] Henk P. Haagsman[a]

Department of Infectious Diseases and Immunology, Division Molecular Host Defense,[a] and Department of Biochemistry and Cell Biology,[b] Faculty of Veterinary Medicine, Utrecht University, Utrecht, The Netherlands

Antifungal mechanisms of action of two cathelicidins, chicken CATH-2 and human LL-37, were studied and compared with the mode of action of the salivary peptide histatin 5 (Hst5). *Candida albicans* was used as a model organism for fungal pathogens. Analysis by live-cell imaging showed that the peptides kill *C. albicans* rapidly. CATH-2 is the most active peptide and kills *C. albicans* within 5 min. Both cathelicidins induce cell membrane permeabilization and simultaneous vacuolar expansion. Minimal fungicidal concentrations (MFC) are in the same order of magnitude for all three peptides, but the mechanisms of antifungal activity are very different. The activity of cathelicidins is independent of the energy status of the fungal cell, unlike Hst5 activity. Live-cell imaging using fluorescently labeled peptides showed that both CATH-2 and LL-37 quickly localize to the *C. albicans* cell membrane, while Hst5 was mainly directed to the fungal vacuole. Small amounts of cathelicidins internalize at sub-MFCs, suggesting that intracellular activities of the peptide could contribute to the antifungal activity. Analysis by flow cytometry indicated that CATH-2 significantly decreases *C. albicans* cell size. Finally, electron microscopy showed that CATH-2 affects the integrity of the cell membrane and nuclear envelope. It is concluded that the general mechanisms of action of both cathelicidins are partially similar (but very different from that of Hst5). CATH-2 has unique features and possesses antifungal potential superior to that of LL-37.

Antimicrobial peptides (AMPs) are host defense molecules that are widely used by a plethora of organisms. These molecules comprise the first line of defense against a broad range of microorganisms, including bacteria, fungi, and even enveloped viruses (1). The antimicrobial activity of AMPs and especially their interactions with membrane components have almost exclusively been studied using either liposomes or bacteria. From these studies three models of peptide-membrane interactions have been proposed (2). In addition, interaction of peptides with intracellular components is thought to constitute an important antimicrobial mode of action. For example, buforin II and tachyplesin have been shown to interact with bacterial DNA (3, 4). Evidence of effects on cellular processes has also been described, e.g., inhibition of protein synthesis by PR-39 and inhibition of enzymatic activity in *Leishmania* spp. by histatin 5 (Hst5) (5–7).

In contrast to the effects on bacteria, the antifungal mode of action of AMPs has been less studied. The different structure and composition of fungal cell walls and membranes compared to those of bacteria suggest that peptides may exert a different mode of action against these microorganisms. Fungal cell membranes contain more zwitterionic phospholipids and sterols, especially in the outer leaflet of the membrane. These lipids make fungal membranes less negatively charged than those of bacteria (8). Cell wall thickness and composition also differ between these organisms. Yeast cell walls contain different polysaccharides such as chitin, β1,3-glucan, and β1,6-glucan, and their thickness ranges from 100 to 200 nm (9). Bacterial cell walls have a thickness from 20 to 80 nm.

One major group of AMPs is the family of cathelicidins. This is a group of highly variable peptides that share a domain known as the cathelin domain at the middle region of the pre-pro-peptide. The carboxy-terminal domain is cleaved to produce a peptide with antimicrobial activity. The active peptides can differ completely in sequence, length, and function between molecules and between species (10). Such variability may well translate into different mechanisms of action of these peptides.

Until now two well-known peptides (LL-37 and Hst5) have been studied for their fungicidal mechanisms against medically relevant fungi. LL-37, the only known cathelicidin peptide produced in humans, is known to have fungicidal activity against *Aspergillus* spp. and *Candida albicans* (11–13). Structurally, LL-37 is amphipathic and has an α-helical conformation with a net positive charge. Its activity at the *C. albicans* cell membrane has been studied by den Hertog and coworkers (11), who found that LL-37 targeted the membrane and caused its complete disruption. In contrast, Hst5, a well-described fungicidal salivary peptide from the histatin family, needs to translocate to the cytosol in order to exert its function (14).

Chicken cathelicidin-2 (CATH-2), one of the four cathelicidins produced by chickens, is a potent antimicrobial peptide (15), but its antifungal activity has not yet been described. Interestingly, the processed peptide does not have any sequence homology with LL-37, and even though both peptides possess an amphipathic α-helical structure, CATH-2 has a pronounced kink due to a proline residue, which divides the peptide into two α-helical segments.

In this study the mechanisms of action against the model or-

Received 1 August 2013 Returned for modification 19 October 2013
Accepted 25 January 2014
Published ahead of print 3 February 2014
Address correspondence to Henk P. Haagsman, h.p.haagsman@uu.nl.
Supplemental material for this article may be found at http://dx.doi.org/10.1128/AAC.01670-13.

doi:10.1128/AAC.01670-13

TABLE 1 Peptide sequences and molecular characteristics

Peptide	Sequence	Length[a]	Charge	H[b]	μH[c]
CATH-2	RFGRFLRKIRRFRPKVTITIQGSARF-NH_2	26	+10	−1.30	0.33
LL-37	LLGDFFRKSKEKIGKEFKRIVQRIKDFLRNLVPRTES	37	+6	−3.48	0.35
Hst5	DSHAKRHHGYKRKFHEKHHSHRGY	24	+5	−4.68	0.09

[a] Length is the number of amino acids.
[b] H, global hydrophobicity as a mean per-residue value.
[c] μH, amphipathicity, determined as the mean hydrophobic moments as described previously (15) using a consensus hydrophobicity scale (16).

ganism *C. albicans* of both human cathelicidin LL-37 and chicken cathelicidin CATH-2 were compared with that of the fungicidal peptide Hst5 using live-cell imaging.

MATERIALS AND METHODS

***C. albicans* strain and growth conditions.** Cultures of *C. albicans* (ATCC 10231) were grown from a frozen glycerol stock in yeast malt (YM; Sigma-Aldrich; Y3752) agar plates. For all experiments, yeasts were cultured at 30°C in 10 ml YM broth until mid-log phase was reached. Cells were washed twice in 5 mM HEPES buffer, pH 7.4. Growth was determined by measuring optical density (OD) at 620 nm and set to 2×10^6 CFU/ml in the same buffer. For minimal fungicidal concentration (MFC) experiments, initial cell density was additionally checked by plating 10-fold dilutions in minimal YM medium.

Peptide production and labeling. Histatin 5 (Hst5), LL-37, and CATH-2 were synthesized and purified as previously described (16–18) (Table 1). Briefly, peptides were synthesized by solid-phase synthesis using 9-fluorenylmethoxy carbonyl (Fmoc) chemistry on a Syro peptide synthesizer (MultiSyntech, Bochum, Germany). Purification of the peptides was performed by reversed-phase high-pressure liquid chromatography (HPLC) on a C_{18} column (Alltech Alltima, Deerfield, IL). Elution of the peptides was done using a linear gradient of 5 to 80% acetonitrile in 0.01% (wt/vol) trifluoroacetic acid. Characterization of the purified peptides was done as previously described (19). Purity was >98%. Fluorescent labels, fluorescein isothiocyanate (FITC) with an emission maximum of 594 nm (Molecular Probes, Life Technologies, United States) or tetramethylrhodamine (TAMRA) with an emission maximum of 583 nm (Novabiochem, Merck Chemical Ltd., United Kingdom), were added during peptide synthesis at the N terminus.

MFC assay. The MFCs of the three peptides were assessed by colony count assays, as previously described (20), with few modifications. Briefly, 25 μl of a 2×10^6-CFU/ml cell suspension, in HEPES buffer (pH 7.4), was incubated for 3 h at 37°C with an equal volume of peptide (0 to 40 μM). Tenfold dilutions in minimal YM medium (1:1,000 dilution of YM in HEPES buffer, pH 7.4) were plated onto YM agar plates and incubated overnight at 37°C. Finally, colonies of surviving yeast were counted. In order to achieve ATP depletion in some of the experiments, *C. albicans* cells were incubated with 5 mM sodium azide before peptide exposure.

ATP release assay. ATP released by the cells during peptide exposure was measured using the ATP determination kit (A22066) from Molecular Probes (Life Sciences, Bleiswijk, The Netherlands). Briefly, a 2×10^6-CFU/ml cell suspension in HEPES buffer (pH 7.4) was incubated with 0.5, 2.5, and 7.5 μM concentrations of each of the three peptides for 5 and 60 min. Samples were centrifuged for 1 min at $1,200 \times g$, and the supernatant was stored on ice for ATP determination as described by the manufacturer. ATP concentrations in the medium without the use of peptides were checked and were below 10 nM (data not shown).

Real-time tracking of CATH-2, LL-37, and Hst5 during *C. albicans* killing. Live-cell imaging experiments were performed as previously described by Jang and coworkers (21) with some modifications. For all experiments, 35-mm culture dishes (FluoroDish; WPI, Sarasota, FL) were coated with concanavalin (Sigma-Aldrich; L7647) at a concentration of 1 mg/ml solution in water, after which 100 μl of a 2×10^6-CFU/ml *C. albicans* cell suspension in HEPES buffer (pH 7.4) was added. Addition of the peptide was done in 50 μl of the buffer containing the specific peptide plus propidium iodide (PI) (Sigma-Aldrich; P4170). The final concentration of PI was 5 μg/ml, while peptide concentrations varied depending on the experiment. In order to investigate the effect of energy depletion on peptide-induced killing, sodium azide (5 mM) was added for 30 min at 30°C before addition of the peptide. In some experiments trypan blue (Sigma-Aldrich; T6146) was used for quenching noninternalized FITC-labeled peptides.

Confocal images were acquired with a Leica SPE-II at the Center for Cell Imaging (CCI), Utrecht University, using 100×/1.4-numerical-aperture objectives. A 488-nm argon laser and a 561-nm diode-pumped solid-state (DPSS) laser were used for simultaneous detection of FITC-labeled peptides and PI, respectively. Additionally, TAMRA-labeled CATH-2 was measured with a 561-nm DPSS laser. ImageJ/Fiji software was used for data analysis; graphs depicting fluorescence versus vacuolar diameter were made using kymographs as described at the Fiji Web page http://fiji.sc/wiki/index.php/Generate_and_exploit_Kymographs.

Cell size reduction by peptide treatment. The effects of CATH-2, LL-37, and Hst5 on *C. albicans* cell size at minimal fungicidal concentrations were measured by both confocal imaging using ImageJ software and flow cytometry. For confocal images, cells were measured before and after 15 min of incubation with the peptide. Statistical analysis was performed using one-way analysis of variance (ANOVA) and Dunnett's multiple-comparison tests. For flow cytometry measurements a BD FACSCalibur machine was used. Comparisons between forward scatter (FSC) and side scatter (SSC) of treated cells and control cells were analyzed by the chi-square test using FlowJo software.

Electron microscopy. Log phase yeast cultures were resuspended to a cell density of 1×10^8 CFU/ml in HEPES buffer, pH 7.4, and treated for 60 min with CATH-2, LL-37, and Hst5 at the MFCs for this cell density: 20 μM, 30 μM, and 20 μM, respectively. Cells were prepared for electron microscopy by permanganate fixation (22). Briefly, cells were washed once with water, resuspended in ice-cold 1.5% $KMnO_4$, and incubated overnight at 4°C while being gently shaken. Subsequently, cells were dehydrated in increasing concentrations of acetone to be later submerged in 33% Spurr's resin for 1 h at room temperature with gentle mixing. Finally, cells were embedded in 100% Spurr's resin, left overnight at room temperature (RT), and then embedded in newly made resin. Samples were heated to 70°C for 2 days to polymerize the resin. Cut sections of 60 nm were stained with uranyl acetate using a Leica EM AC20 system. Imaging was done using a FEI Tecnai 12 electron microscope at 80 kV. Cells were selected randomly at low magnification and zoomed to observe changes in membrane structures. For each parameter at least 30 cells were included in the analysis.

RESULTS

Candidacidal activity of CATH-2. The candidacidal activities of CATH-2, LL-37, and Hst5 were determined by colony count assays (Fig. 1). These assays showed a 1,000-fold reduction in viable yeast cells at 1.25 μM CATH-2 and complete killing of all *C. albicans* cells at 2.5 μM (MFC). Hst5 exhibited candidacidal activity similar to that of CATH-2, having an MFC of 5 μM. LL-37 had a slightly higher MFC of 10 μM under these experimental conditions. For live-cell imaging experiments, the MFCs were used, but

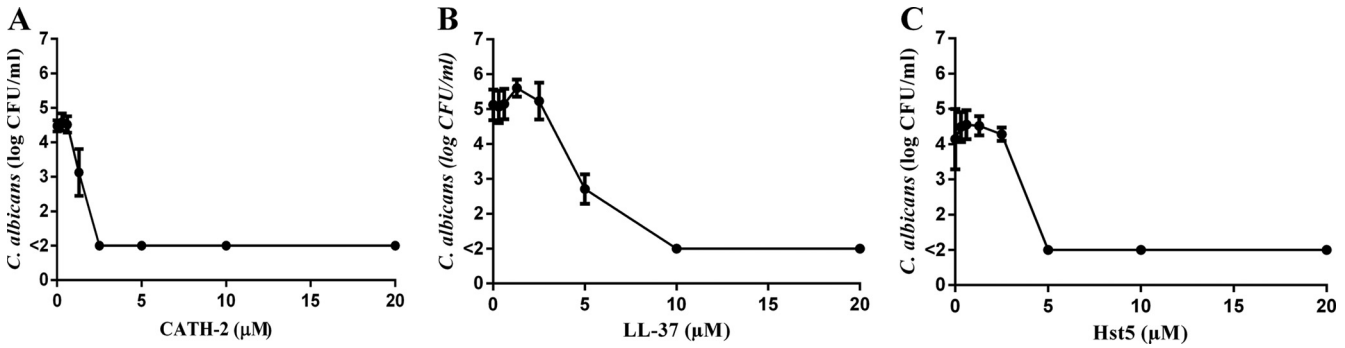

FIG 1 Candidacidal activity of CATH-2 (A), LL-37 (B), and Hst5 (C). The minimum fungicidal concentrations (MFC) were assessed by colony count assays. Shown are the averages and standard errors of the means (SEM) of four independent experiments.

not for Hst5. For this peptide, a concentration of 5 μM was used in order to observe killing kinetics at a slower pace.

Peptides cause vacuolar expansion and PI influx. In order to compare the killing kinetics of the three AMPs, confocal live-cell images using FITC-labeled or unlabeled peptides and propidium iodide (PI) as a permeability indicator were recorded. Labeling of peptides did not have an effect on MFC values (see Fig. S1 in the supplemental material). Several initial effects were observed after peptide addition (Fig. 2). For CATH-2 a small increase in intracellular localization of PI, indicative of membrane permeabilization, was observed at the MFC (2.5 μM) within 2 min of contact. Subsequently, the central vacuole of *C. albicans* expanded (Fig. 2, differential interference contrast [DIC] images), and a 200-fold increase in PI intensity throughout the cytosol was observed. Intensity measurements of PI influx relative to vacuolar increase showed that both processes occurred simultaneously and seemed to be linked (Fig. 2A). During this process cells shrank considerably, especially after the central vacuole imploded (see Movie S1 in the supplemental material). To analyze this decrease in cell size, we measured cell area before and after 15 min of incubation with peptides when cells were already permeable to PI. A significant decrease of 20% in cell area was observed for CATH-2-treated fungal cells (see Fig. S2). To better quantify these differences, samples were analyzed by flow cytometry, where sizes (FSC) and cell

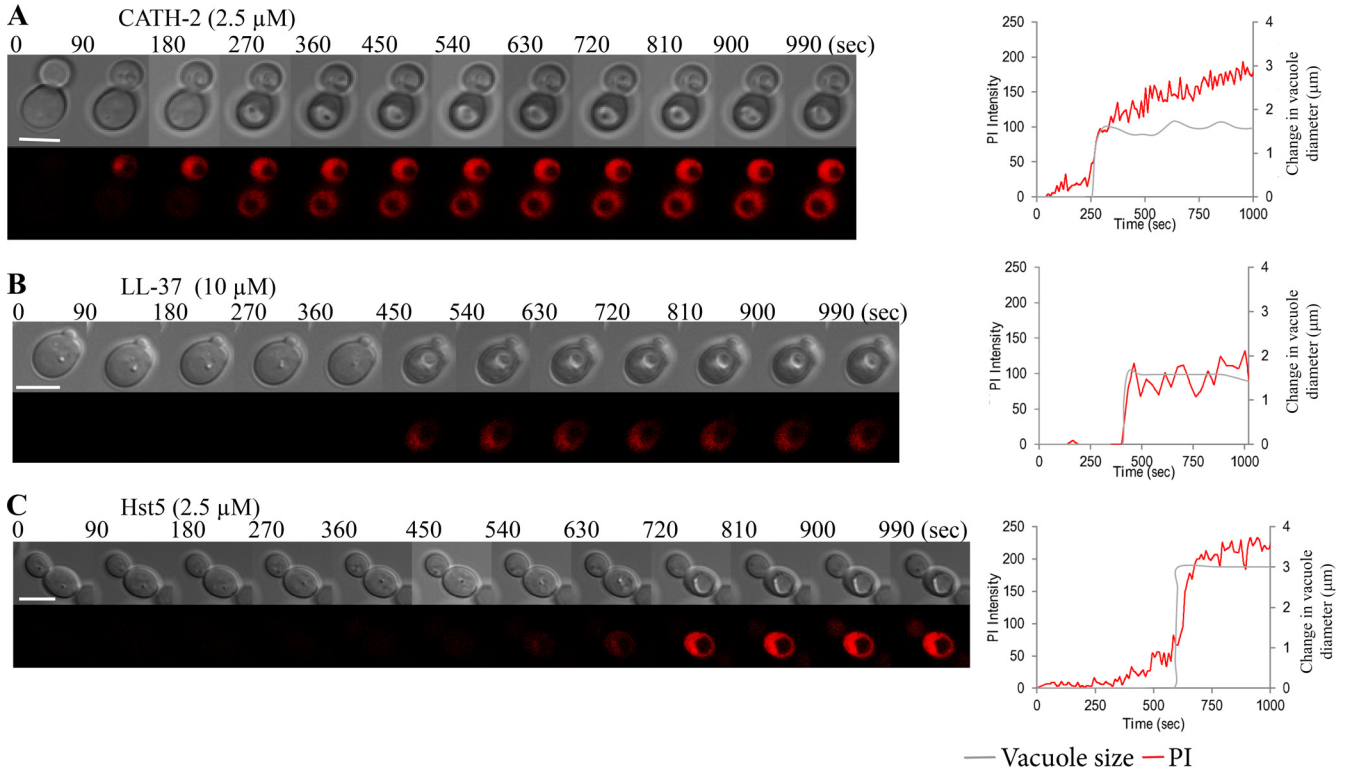

FIG 2 Live-cell imaging of peptide-induced killing of *C. albicans* visualized by propidium iodide (PI) influx. Montage pictures show changes in cell structure (DIC channel) and PI influx during peptide killing at MFC. Bars, 5 μm. Right panels show PI influx plotted against vacuolar expansion for each cell. PI influx increased 200-fold with concomitant vacuolar expansion and initiated at different time points after addition of the peptide. Depicted cells are representative of more than 3 separate experiments for each peptide. For measuring purposes the initial diameter of the vacuole was arbitrarily set to zero.

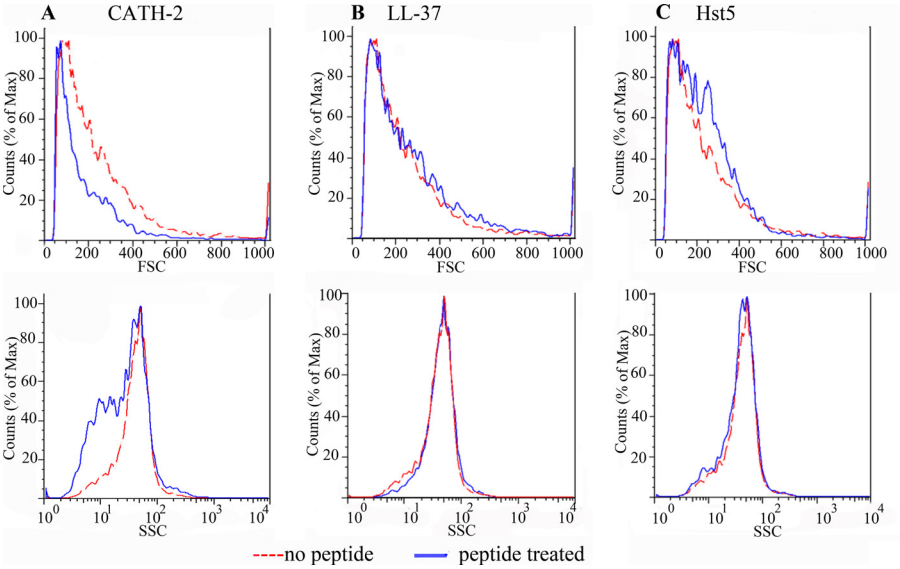

FIG 3 CATH-2-induced cell shrinkage. *C. albicans* size and morphology changes were measured by flow cytometry after 15 min of incubation with CATH-2 (A), LL-37 (B), or Hst5 (C) at MFC. CATH-2 was the only peptide that affected cell size (FSC) and granularity (SSC) of *C. albicans* after treatment ($P < 0.001$).

complexities (SSC) were compared. These experiments indicated that CATH-2 treatment produced a significant decrease in cell size and cell complexity ($P < 0.001$) (Fig. 3).

Exposing *C. albicans* to a higher concentration of CATH-2 (7.5 μM) resulted in a similar order of events, although PI influx and vacuolar expansion occurred faster, while sub-MFC CATH-2 concentrations resulted in a reduced number of cells showing the described effects. Similar to CATH-2 treatment, treatment of *C. albicans* with 10 μM LL-37 and 2.5 μM Hst5 (MFC values) triggered PI influx at around 450 and 540 s, respectively. This event was also coupled to vacuolar expansion (Fig. 2B and C), as observed for CATH-2; however, no decrease in cell size was observed with either cell area or flow cytometry measurements (Fig. 3).

CATH-2-induced ATP release is immediate after contact. The observed effects of vacuolar expansion and PI influx indicate that membrane permeabilization is a major factor in the candidacidal mechanism, in agreement with a previous report (11). To increase our understanding of this matter, peptide-induced ATP leakage was determined 5 and 60 min after addition (Fig. 4). Interestingly, at the MFC CATH-2 triggered ATP release soon after contact and this release did not increase after 60 min of exposure. In contrast, sub-MFC concentrations show an increase in ATP release only after 60 min of exposure. Furthermore, lower ATP levels were measured when higher peptide concentrations were used. For LL-37 the profile observed was similar to that for CATH-2 with the exception that high and immediate ATP releases were observed at 2.5 μM, which is 2-fold lower than the MFC, while at the MFC (5 to 10 μM) a decrease in ATP release is observed. These observations differ from those for Hst5, where released ATP increased in time and was directly related to the peptide concentration used.

Localization of CATH-2, LL-37, and Hst5 during *C. albicans* killing. FITC-labeled CATH-2 (at MFC of 2.5 μM) localized to the cell surface immediately after addition, with more-intense staining at the cell poles (Fig. 5). Surface fluorescence intensity increased 200-fold in a few seconds and decreased significantly over the first minutes, which cannot be explained by a rapid internalization of CATH-2. At MFCs, almost no cells showed vacuolar collapse before 30 min and no intracellular CATH-2 was observed. Only after quenching of extracellular fluorescent CATH-2

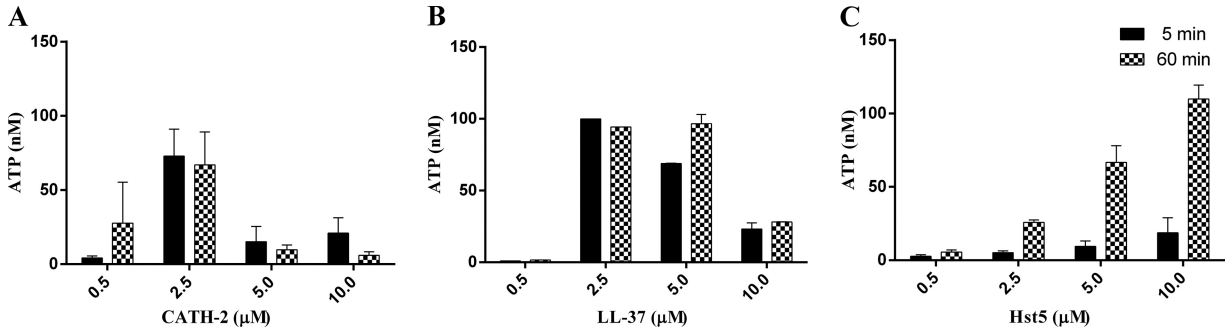

FIG 4 Peptide-induced ATP release. Graphs shows ATP concentrations in the culture medium (averages and SEM of three independent experiments performed in duplicate) at 5 and 60 min after contact with each peptide. While cathelicidins (A and B) induce a sudden release of ATP at MFC, the effect of Hst5 (C) is gradual over time and proportional to the peptide concentration used.

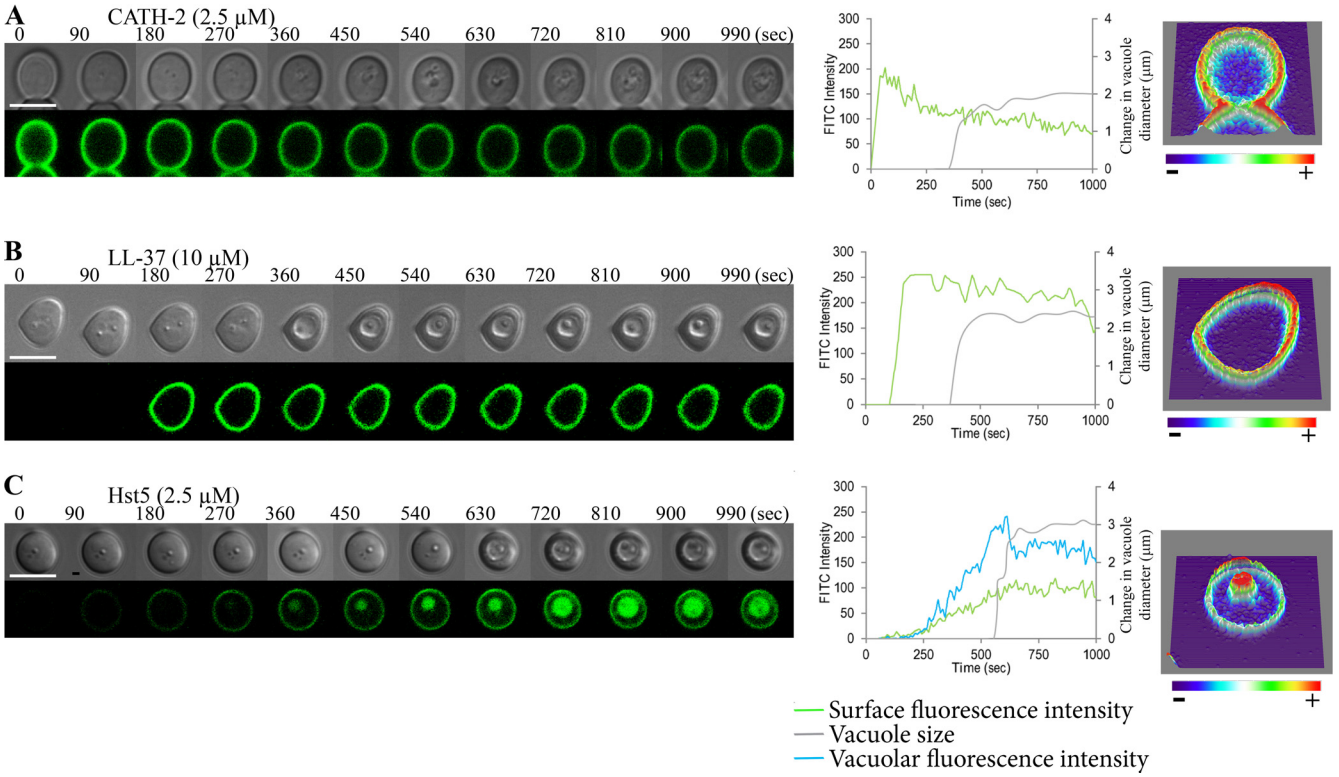

FIG 5 Localization of FITC-labeled peptides. (Left) Montage pictures of confocal live-cell imaging movies depicting FITC-labeled peptides. Bars, 5 μm. (Middle) Plots for membrane and cytosol fluorescence versus vacuolar expansion of each representative cell. (Right) Three-dimensional plot of each cell after 90 s (CATH-2), 180 s (LL-37), and 360 s (Hst5). The color gradient indicates changes in intensity, showing sites where peptide concentration is the highest in red.

was the internalized peptide faintly visible in specific sites inside the cell (Fig. 6). Similar effects were shown when TAMRA-labeled CATH-2 was used, proving that peptide labeling was not interfering with localization.

At concentrations 3 times greater than the MFC, approximately 90% of cells suffered vacuolar collapse after 20 min of imaging, and soon after cytosolic CATH-2 was visible (see Movie S1 in the supplemental material). Localization after entry was mainly seen in patches near the membrane (especially near the cell poles). Furthermore, it was possible to follow peptide entry through one of the poles in a few cells (see Movie S2), although it could not be determined whether these were isolated events or reflect the general mechanism of peptide entry. Similar experiments using FITC-labeled LL-37 showed that this peptide fol-

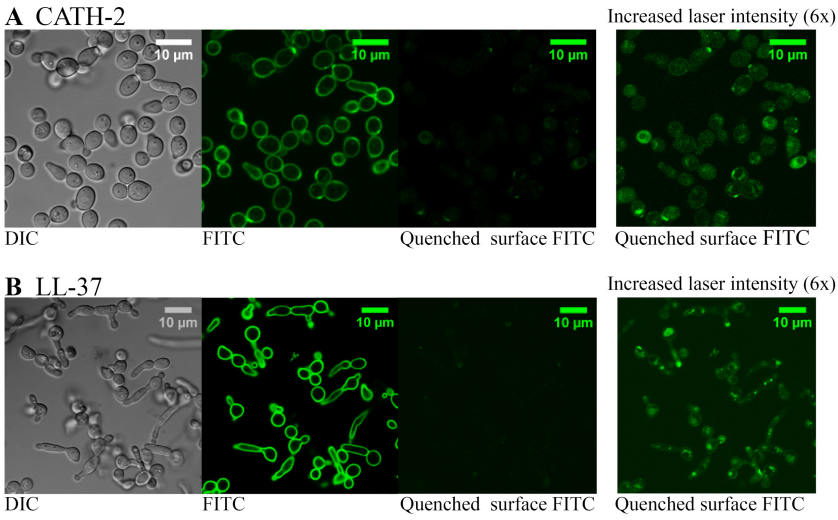

FIG 6 Quenching of surface FITC-labeled peptide. CATH-2 (A) and LL-37 (B) were added at MFC. Immediately after trypan blue was added, the surface signal was blocked, and by increasing 6-fold the laser intensity (right panels) it was possible to visualize the internalized peptide.

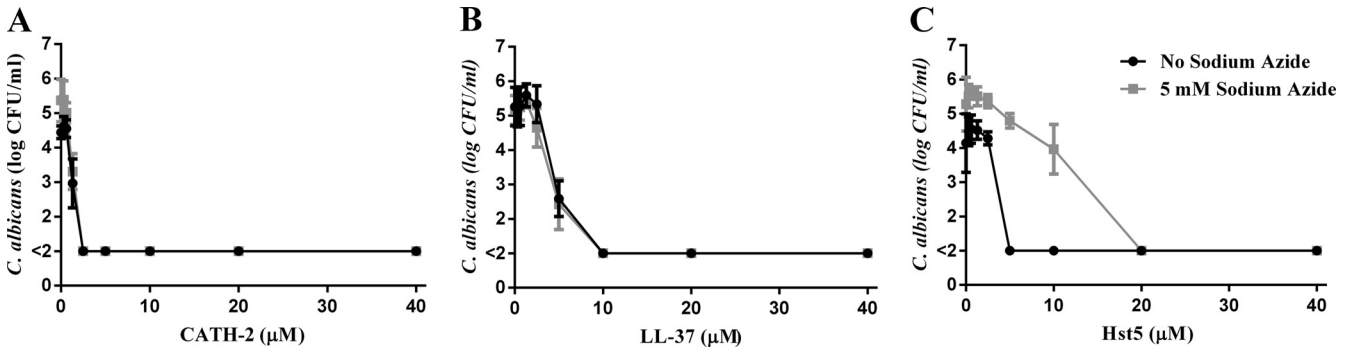

FIG 7 Effect of azide on the MFCs of CATH-2 (A), LL-37 (B), and Hst5 (C). Results are shown as the means and SEM of three separate experiments. Hst5 activity is significantly affected by sodium azide.

lowed the same steps and localized similarly to CATH-2 during peptide entry. However, localization of Hst5 greatly differed from that of CATH-2 and LL-37. At MFCs, Hst5 localization at the cell surface increased gradually, and at the same time a similar increase in the cytosol and vacuole was observed (Fig. 5C).

CATH-2 and LL-37 candidacidal activities are not affected by sodium azide. The candidacidal activities of CATH-2 and LL-37 were not dependent on the energy status of the cells. In contrast, the activity of Hst5 was completely inhibited by azide, a poison that reduces ATP levels of the cells (Fig. 7). To study the mechanism in more detail, cells were observed by confocal live-cell imaging. In the presence of azide, CATH-2 still permeabilized the cells and induced vacuolar expansion, similar to the effects in the absence of azide. Distribution and internalization of CATH-2 did not alter after azide treatment (Fig. 8). In contrast, PI influx in Hst5-treated cells was completely inhibited by azide and no peptide localized inside the vacuole or in the cytosol.

Electron microscopy reveals that CATH-2, LL-37, and Hst5 have distinct effects on *C. albicans* at MFC. Analysis by transmission electron microscopy (TEM) of *C. albicans* treated with each of the three peptides showed CATH-2 to have the most pronounced effects on membranes. The clearest effect produced by CATH-2 was detachment of the plasma membrane (PM) from the cell wall and the formation of pockets close to the cell poles (Fig. 9B). In other cases it was possible to observe breakage of extended areas of the cell membrane and areas with thicker membrane portions. Internally, the nuclear membrane was clearly disrupted in almost all cells, but mitochondria did not seem to be affected. In addition to the membrane effect, cell wall integrity was also affected, as shown by detachment of the cellular wall.

For LL-37 the effects observed were less clear (Fig. 9C). Some cells presented membrane detachment similar to what was seen for CATH-2, but cell wall and internal membranes were not visibly disrupted. No effects of Hst5 were visible by electron microscopy, neither effects on membranes nor changes on the cell wall (Fig. 9D).

DISCUSSION

In the present study the antifungal mechanisms of two cathelicidins were compared to that of Hst5, a well-known candidacidal peptide. Although all three peptides have comparable cationic and amphipathic features, there are also notable differences between them. No apparent sequence homology between the three peptides is present, and LL-37 is also significantly bigger than CATH-2 and Hst5. Structurally, LL-37 and Hst5 form a close-to-

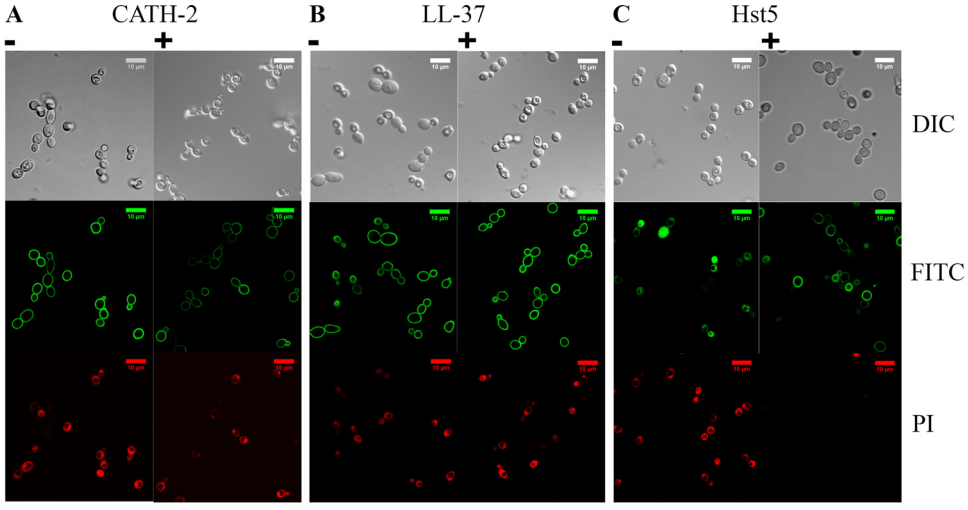

FIG 8 Energy depletion by sodium azide affects the activity of Hst5 but not of LL-37 and CATH-2. Peptide localization in *C. albicans* without (−) and with (+) sodium azide is shown.

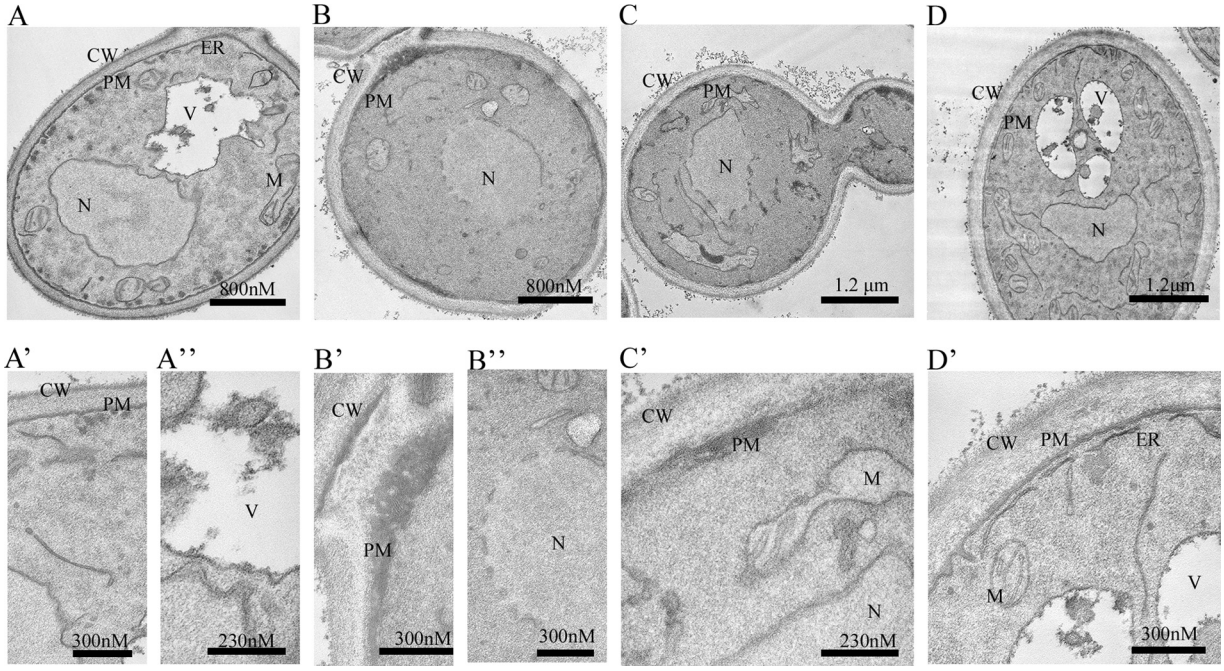

FIG 9 Peptide-induced morphological changes observed by TEM. Shown are TEM pictures from representative cells for each peptide treatment and control. (A to A″) Control; (B to B″) CATH-2; (C and C′) LL-37; (D and D′) Hst5. CATH-2 induced detachment of the plasma membrane (PM) from the cell wall (CW) and disruption of nuclear envelope. LL-37 produces similar membrane effects but to a lesser extent, while Hst5 had no observable effects on cell membranes. M, mitochondria; N, nuclei; V, vacuole; ER, endoplasmic reticulum.

perfect helix, while CATH-2 contains a proline-induced kink in the middle of the helix (19, 23).

One of the clearest phenomena for all three peptide treatments was the increase in vacuolar size. As described by Jang and coworkers (21), vacuolar resizing is related to osmotic stress and likely reflects leakage of cytosolic ions. The simultaneous influx of PI supports this hypothesis. Contrary to what we observed, the study by Jang et al. showed that PI entry happens after vacuolar expansion. This difference in the sequence of events might be attributed to differences in the peptide concentrations used. In this study we used the MFC or concentrations close to the MFC, while 10-fold higher concentrations were used in the above-mentioned study.

After the initial cytosolic influx of PI, its concentration increases about 200-fold when the vacuole stops expanding. The increase in fluorescence can be related to a decrease in cytosolic volume due to vacuolar expansion and an increase in permeabilization due to membrane disruption by the peptide. In parallel to PI efflux, loss of ions occurs as early as 5 min after peptide contact. Interestingly, both cathelicidins induce ATP release rapidly at low concentrations, but this was no longer measurable at high peptide concentrations, contrary to what is seen for Hst5. The decrease in measurable ATP at high cathelicidin concentrations suggests rapid degradation of ATP by enzymes released in the medium due to membrane damage. If this is the case, lower concentrations might induce transient permeabilization, while high concentrations might allow gross disruption of the membranes, leading to enzyme leakage and rapid cell death.

It was also interesting to observe, in parallel to the permeabilization effects, a loss in cell volume during killing by CATH-2, which did not occur with the other two peptides (Fig. 3). Barns and Weisshaar described a similar effect in the Gram-positive bacterium *Bacillus subtilis* if exposed to concentrations higher than MICs of LL-37 (24). In their study loss of turgor and possibly loss of transmembrane potential were the likely causes of cell shrinkage, an effect from which the cells could not recover. It is possible that CATH-2-induced cell shrinkage has similar causes. This observation is in line with our results, obtained by transmission electron microscopy and by flow cytometry, that showed shrinkage of the cell membrane and its detachment from the cell wall.

It is still unclear whether, apart from the effects of cathelicidins on membranes during killing, binding to intracellular targets is part of their antimicrobial activity. For LL-37 and CATH-2, the strong membrane staining during the killing process would suggest that direct membrane permeabilization is the main mechanism of their action. However, it is clear from our experiments that small amounts of peptides are present intracellularly, even before PI influx and vacuolar expansion take place. If that is the case, the actual transportation of peptides across the membrane would be an energy-independent process, since the addition of azide did not prevent their candidacidal activity. It is possible that a relatively high concentration of peptides at the membrane is required for the peptides to traverse the cell boundaries. Intracellular localization of peptides increased drastically after *C. albicans* vacuolar implosion (see Movie S3 in the supplemental material), but this could be a secondary effect and not the cause of killing. In line with this notion, intracellular targets for the antibacterial activity of LL-37 have been described, while it was still localized mainly at the membrane (25). The mechanism of the candidacidal action of Hst5 has been studied in detail (21). Its effect is attributed to several changes in the cell due to the lack of internal ATP (26, 27), though in order to produce these changes Hst5 needs to

translocate to the cytosol of the cell. Indeed, we found that the effect of Hst5 but not that of the cathelicidins can be blocked by sodium azide, which inhibits ATP-dependent internalization pathways and also possibly rigidifies the cellular membrane due to actin depolymerization (26).

Differences in the cell surface of the yeast *C. albicans* compared to that of bacteria do not seem to affect the mechanism of action of cathelicidins. Both in the yeast and in bacteria the membrane was the main target. Furthermore, LL-37 and CATH-2 are active at concentrations similar to those we used in this study against several bacteria (25, 28, 29). In contrast, mammalian cells seem to differ enough to avoid the cytotoxic effects due to membrane permeabilization of CATH-2 (28, 30). Differences in phospholipid composition and sterol subtypes (cholesterol versus ergosterol) between mammalian and fungal membranes or the overall negative charge could be the cause of this selectivity (8).

Our results indicate that, even though membrane destabilization seems to be the most prominent effect of the candidacidal activities of cathelicidins, the importance of internal targets for cathelicidins cannot be ruled out yet. The rapid onset of effects on internal membranes at the MFC suggests additional mechanisms of action of cathelicidins. The internalization of cathelicidins at low concentrations that do not induce membrane permeabilization is in line with this notion. It may very well be possible that the concentrations of cathelicidins do not need to reach the MFC to exert an effect that renders the organisms vulnerable to immunological attack.

ACKNOWLEDGMENTS

This work was supported by a Program Grant (RGP0016/2009-C) of the Human Frontier Science Program.

We thank Aimee Uwland for her help in the initial stages of the project and George Posthuma from the Cell Microscopy Center, Department of Cell Biology, University Medical Center Utrecht, The Netherlands, for technical support with the electron microscopy work.

REFERENCES

1. **Zasloff M.** 2002. Antimicrobial peptides of multicellular organisms. Nature **415:**389–395. http://dx.doi.org/10.1038/415389a.
2. **Brogden KA.** 2005. Antimicrobial peptides: pore formers or metabolic inhibitors in bacteria? Nat. Rev. Microbiol. **3:**238–250. http://dx.doi.org/10.1038/nrmicro1098.
3. **Yonezawa A, Kuwahara J, Fujii N, Sugiura Y.** 1992. Binding of tachyplesin I to DNA revealed by footprinting analysis: significant contribution of secondary structure to DNA binding and implication for biological action. Biochemistry **31:**2998–3004. http://dx.doi.org/10.1021/bi00126a022.
4. **Park CB, Kim HS, Kim SC.** 1998. Mechanism of action of the antimicrobial peptide buforin II: buforin II kills microorganisms by penetrating the cell membrane and inhibiting cellular functions. Biochem. Biophys. Res. Commun. **244:**253–257. http://dx.doi.org/10.1006/bbrc.1998.8159.
5. **Boman HG, Agerberth B, Boman A.** 1993. Mechanisms of action on Escherichia coli of cecropin P1 and PR-39, two antibacterial peptides from pig intestine. Infect. Immun. **61:**2978–2984.
6. **Andreu D, Rivas L.** 1998. Animal antimicrobial peptides: an overview. Peptide Sci. **47:**415. http://dx.doi.org/10.1002/(SICI)1097-0282(1998)47:6<415::AID-BIP2>3.0.CO;2-D.
7. **Luque-Ortega JR, van't Hof W, Veerman EC, Saugar JM, Rivas L.** 2008. Human antimicrobial peptide histatin 5 is a cell-penetrating peptide targeting mitochondrial ATP synthesis in Leishmania. FASEB J. **22:**1817–1828. http://dx.doi.org/10.1096/fj.07-096081.
8. **Yeaman MR, Yount NY.** 2003. Mechanisms of antimicrobial peptide action and resistance. Pharmacol. Rev. **55:**27–55. http://dx.doi.org/10.1124/pr.55.1.2.
9. **Peckys DB, Mazur P, Gould KL, de Jonge N.** 2011. Fully hydrated yeast cells imaged with electron microscopy. Biophys. J. **100:**2522–2529. http://dx.doi.org/10.1016/j.bpj.2011.03.045.
10. **Bals R, Wilson JM.** 2003. Cathelicidins—a family of multifunctional antimicrobial peptides. Cell. Mol. Life Sci. **60:**711–720. http://dx.doi.org/10.1007/s00018-003-2186-9.
11. **den Hertog AL, van Marle J, van Veen HA, Van't Hof W, Bolscher JG, Veerman EC, Nieuw Amerongen AV.** 2005. Candidacidal effects of two antimicrobial peptides: histatin 5 causes small membrane defects, but LL-37 causes massive disruption of the cell membrane. Biochem. J. **388:**689–695. http://dx.doi.org/10.1042/BJ20042099.
12. **Mania D, Hilpert K, Ruden S, Fischer R, Takeshita N.** 2010. Screening for antifungal peptides and their modes of action in Aspergillus nidulans. Appl. Environ. Microbiol. **76:**7102–7108. http://dx.doi.org/10.1128/AEM.01560-10.
13. **Benincasa M, Scocchi M, Pacor S, Tossi A, Nobili D, Basaglia G, Busetti M, Gennaro R.** 2006. Fungicidal activity of five cathelicidin peptides against clinically isolated yeasts. J. Antimicrob. Chemother. **58:**950–959. http://dx.doi.org/10.1093/jac/dkl382.
14. **Ruissen AL, Groenink J, Helmerhorst EJ, Walgreen-Weterings E, Van't Hof W, Veerman EC, Nieuw Amerongen AV.** 2001. Effects of histatin 5 and derived peptides on Candida albicans. Biochem. J. **356:**361–368. http://dx.doi.org/10.1042/0264-6021:3560361.
15. **Cuperus T, Coorens M, van Dijk A, Haagsman HP.** 2013. Avian host defense peptides. Dev. Comp. Immunol. **41:**352–369. http://dx.doi.org/10.1016/j.dci.2013.04.019.
16. **Eisenberg D, Weiss RM, Terwilliger TC.** 1982. The helical hydrophobic moment: a measure of the amphiphilicity of a helix. Nature **299:**371–374. http://dx.doi.org/10.1038/299371a0.
17. **Tossi A, Sandri L, Giangaspero A.** 2000. Amphipathic, alpha-helical antimicrobial peptides. Biopolymers **55:**4–30. http://dx.doi.org/10.1002/1097-0282(2000)55:1<4::AID-BIP30>3.0.CO;2-M.
18. **Bikker FJ, Kaman-van Zanten WE, de Vries-van de Ruit AM, Voskamp-Visser I, van Hooft PA, Mars-Groenendijk RH, de Visser PC, Noort D.** 2006. Evaluation of the antibacterial spectrum of drosocin analogues. Chem. Biol. Drug Des. **68:**148–153. http://dx.doi.org/10.1111/j.1747-0285.2006.00424.x.
19. **van Dijk A, Molhoek EM, Veldhuizen EJ, Bokhoven JL, Wagendorp E, Bikker F, Haagsman HP.** 2009. Identification of chicken cathelicidin-2 core elements involved in antibacterial and immunomodulatory activities. Mol. Immunol. **46:**2465–2473. http://dx.doi.org/10.1016/j.molimm.2009.05.019.
20. **van Dijk A, Veldhuizen EJ, Kalkhove SI, Tjeerdsma-van Bokhoven JL, Romijn RA, Haagsman HP.** 2007. The beta-defensin gallinacin-6 is expressed in the chicken digestive tract and has antimicrobial activity against food-borne pathogens. Antimicrob. Agents Chemother. **51:**912–922. http://dx.doi.org/10.1128/AAC.00568-06.
21. **Jang WS, Bajwa JS, Sun JN, Edgerton M.** 2010. Salivary histatin 5 internalization by translocation, but not endocytosis, is required for fungicidal activity in Candida albicans. Mol. Microbiol. **77:**354–370. http://dx.doi.org/10.1111/j.1365-2958.2010.07210.x.
22. **Stevens B, White JG.** 1979. Computer reconstruction of mitochondria from yeast. Methods Enzymol. **56:**718–728. http://dx.doi.org/10.1016/0076-6879(79)56064-9.
23. **Johansson J, Gudmundsson GH, Rottenberg ME, Berndt KD, Agerberth B.** 1998. Conformation-dependent antibacterial activity of the naturally occurring human peptide LL-37. J. Biol. Chem. **273:**3718–3724. http://dx.doi.org/10.1074/jbc.273.6.3718.
24. **Barns KJ, Weisshaar JC.** 2013. Real-time attack of LL-37 on single Bacillus subtilis cells. Biochim. Biophys. Acta **1828:**1511–1520. http://dx.doi.org/10.1016/j.bbamem.2013.02.011.
25. **Sochacki KA, Barns KJ, Bucki R, Weisshaar JC.** 2011. Real-time attack on single Escherichia coli cells by the human antimicrobial peptide LL-37. Proc. Natl. Acad. Sci. U. S. A. **108:**E77–E81. http://dx.doi.org/10.1073/pnas.1101130108.
26. **Veerman EC, Valentijn-Benz M, Nazmi K, Ruissen AL, Walgreen-Weterings E, van Marle J, Doust AB, van't Hof W, Bolscher JG, Amerongen AV.** 2007. Energy depletion protects Candida albicans against antimicrobial peptides by rigidifying its cell membrane. J. Biol. Chem. **282:**18831–18841. http://dx.doi.org/10.1074/jbc.M610555200.
27. **Koshlukova SE, Lloyd TL, Araujo MW, Edgerton M.** 1999. Salivary histatin 5 induces non-lytic release of ATP from Candida albicans leading to cell death. J. Biol. Chem. **274:**18872–18879. http://dx.doi.org/10.1074/jbc.274.27.18872.
28. **van Dijk A, Tersteeg-Zijderveld MH, Tjeerdsma-van Bokhoven JL,**

Jansman AJ, Veldhuizen EJ, Haagsman HP. 2009. Chicken heterophils are recruited to the site of Salmonella infection and release antibacterial mature cathelicidin-2 upon stimulation with LPS. Mol. Immunol. **46:** 1517–1526. http://dx.doi.org/10.1016/j.molimm.2008.12.015.

29. **Veldhuizen EJ, Brouwer EC, Schneider VA, Fluit AC.** 2013. Chicken cathelicidins display antimicrobial activity against multiresistant bacteria without inducing strong resistance. PLoS One **8:**e61964. http://dx.doi.org/10.1371/journal.pone.0061964.
30. **Molhoek EM, van Dijk A, Veldhuizen EJ, Haagsman HP, Bikker FJ.** 2011. A cathelicidin-2-derived peptide effectively impairs Staphylococcus epidermidis biofilms. Int. J. Antimicrob. Agents. **37:**476–479. http://dx.doi.org/10.1016/j.ijantimicag.2010.12.020.